A Density Functional Study of Ethene Hydrogenation Reactions Catalyzed by Titanocene Complexes

Jung-Goo Lee,* Ho Young Jeong, Young Hoon Ko, Jee Hwan Jang, and Hosull Lee

Contribution from the KUMHO Chemical Laboratories, P.O. Box 64, Yuseong, Taejon 305−600, South Korea

Received June 1, 1999. Revised Manuscript Received May 4, 2000

Abstract: Density functional calculations have been carried out to investigate the mechanisms of ethene hydrogenation reactions catalyzed by four different titanocene complexes, $Cp_2Ti(CO)_2$, $Cp_2Ti(CH_3)_2$, $Cp_2Ti(C_6H_5)_2$, and $Cp_2Ti(p\text{-}C_6H_4CH_3)_2$ (Cp: cyclopentadienyl group = η^5-C_5H_5). The molecular geometries of the ground and transition states in these reactions have also been evaluated. The hybrid density functional method B3PW91 showed the best agreement with the experimental geometries of $Cp_2Ti(CO)_2$. B3PW91 computations of activation parameters for the thermal decomposition of Cp_2TiMe_2 also showed good agreement with previous experimental data on a similar complex, $(\eta^5\text{-}C_5Me_5)_2TiMe_2$. Ethene hydrogenation by $Cp_2Ti(CO)_2$ proceeds in the following order: first and second bond dissociations of Ti−C(CO) bonds followed by the formation of Cp_2TiH_2 from ($Cp_2Ti + H_2$) and then ethene hydrogenation by Cp_2TiH_2. B3PW91 computations indicated that continuous heating of the system is necessary until the activation barrier of ethene hydrogenation by Cp_2TiH_2 is overcome. This is because the first three reactions occur nonspontaneously (at room temperature, ΔG = 18.4, 12.8, and 7.4 kcal/mol, respectively). This qualitative finding is supported by the corresponding experimental temperature (= 65 °C). For the Cp_2TiR_2 catalysts (where R = methyl, phenyl, and tolyl groups), ethene hydrogenation is found to be of first and second σ bond metathesis for the Ti−C(R) bond and H−H bond to form Cp_2TiH_2, followed by ethene hydrogenation by Cp_2TiH_2. Another ethene hydrogenation begins with the first σ bond metathesis for the Ti−C(R) bond and H−H bond, which is followed by the reductive elimination of RH to form Cp_2Ti, the formation of Cp_2TiH_2, and then ethene hydrogenation by Cp_2TiH_2. In both hydrogenation reactions for the Cp_2TiR_2 catalysts, first σ bond metathesis reactions are found to be rate-determining and the $\Delta G^{\ddagger}$s are calculated to be very close in value ($\Delta G^{\ddagger}$ = 31.5 kcal/mol, with R = CH_3; 32.0 kcal/mol, with R = C_6H_5; and 32.6 kcal/mol, with R = $C_6H_4CH_3$, at room temperature). Contrary to the case of $Cp_2Ti(CO)_2$, all reactions by Cp_2TiR_2 (except for the formation of Cp_2TiH_2) are spontaneous, or ΔGs < 0. The ΔGs in the case of Cp_2TiR_2 are found to be sufficient to overcome the activation Gibbs free energies for the subsequent reactions. Only the activation barrier for first σ bond metathesis by Cp_2TiR_2 has to be overcome by a proper temperature control. Since the ΔS for first σ bond metathesis is negative, the hydrogenation by Cp_2TiR_2 takes place below room temperature. These results are supported by the corresponding experimental temperature (= 0 °C). Alternative hydrogenation pathways through Ti−C(CO) bond dissociation of $Cp_2Ti(CO)(H_2)$ or through α-H abstraction of $Cp_2Ti(CH_3)_2$ have also been discussed.

Introduction

Tetravalent group 4 metallocenes (Cp_2MR_2), soluble hydrogenation catalysts, have been extensively studied[1] since the initial report on them in the 1950s.[2] Recently, soluble metallocene complexes have been used successfully for the hydrogenation of conjugated diolefin polymers.[3] The hydrogenated polymers show superior physical properties related to heat, oxidation, and ozone resistances compared with those of the unsaturated polymers. Temperature control of the hydrogenation reactions is essential to achieve effective industrial production of the saturated polymers. Therefore, it is important to understand the mechanism of the hydrogenation process. Brintzinger and co-workers[4] reported the hydrogenation of ethene using $Cp_2Ti(CO)_2$, where Cp_2Ti or $(Cp_2Ti)_2$ was postulated as an intermediate. The Cp_2Ti or $(Cp_2Ti)_2$ reacts with H_2 to form a dimer, $(Cp_2TiH)_2$, which subsequently hydrogenates ethene (see Scheme 1). The Ti−C bonds of other catalysts such as $Cp_2Ti(CH_3)_2$, $Cp_2Ti(C_2H_5)_2$, and $Cp_2Ti(\eta^3\text{-}C_5H_9)$ are also believed to be initially cleaved during the hydrogenation reactions.[4]

However, a detailed mechanism for the hydrogenation is still lacking. For example, $(Cp_2TiH)_2$ is formed as an intermediate,

* To whom correspondence should be addressed. E-mail: jglee@www.kkpc.re.kr.

(1) (a) Wilkinson, G.; Pauson, P. L.; Birmingham, J. M.; Cotton, F. A. *J. Am. Chem. Soc.* **1953**, *75*, 1011. (b) Wailes, P. C.; Coutts, R. S. P.; Wegold, H. *Organometallic Chemistry of Titanium, Zirconium and Hafnium*; Academic Press: New York, 1974.

(2) Wilkinson, G.; Birmingham, J. M. *J. Am. Chem. Soc.* **1954**, *76*, 4281

(3) For example, see (a) Kishimoto, Y.; Morita, H. U.S. Patent 4,501,-857, 1985. (b) Kishimoto, Y.; Masubuchi, T. U.S. Patent 4,673,714, 1987. (c) Kato, K.; Kishimoto, Y.; Kameda, T. JP 01289805 A, 1989. (d) Zhang, Y.; Liao, S.; Xu, Y. *J. Organomet. Chem.* **1990**, *382*, 69. (e) Teramoto, T.; Goshima, K.; Takeuchi, M. U.S. Patent 4,980,421, 1990. (f) Hoxmeier, R. J. U.S. Patent 5,013,798, 1991. (g) Chamberlain, L. R.; Gibler, C. J. U.S. Patent 5,039,755, 1991. (h) Kato, K.; Kishimoto, Y. JP 04096904 A, 1990. (i) Kato, K.; Kishimoto, Y. JP 04096905 A, 1992. (j) Kitagawa, Y.; Hattori, Y. JP 04227648 A, 1992. (k) Goodwin, D. E. U.S. Patent 5,166,277, 1992. (l) Chamberlain, L. R. U.S. Patent 5,206,307, 1993. (m) Gibler, C J. U.S. Patent 5,334,566, 1994. (n) Willis, C. L. U.S. Patent 5,521,254, 1996. (o) Ferrer, M. D. P.; Calle, J. A. B. U.S. Patent 5,583,185, 1996. (p) Ko, Y. H.; Kim, H. C.; Cho, S. D. U.S. Patent 5,753,778, 1998. (q) Ko, Y. H.; Lee, J.-G.; Kim, J. Y. JP 112903471, 1999.

(4) Bercaw, J. E.; Marvich, R. H.; Bell, L. G.; Brintzinger, H. H. *J. Am. Chem. Soc.* **1972**, *94*, 1219.

10.1021/ja991799l CCC: $19.00
Published on Web 06/24/2000

Scheme 1

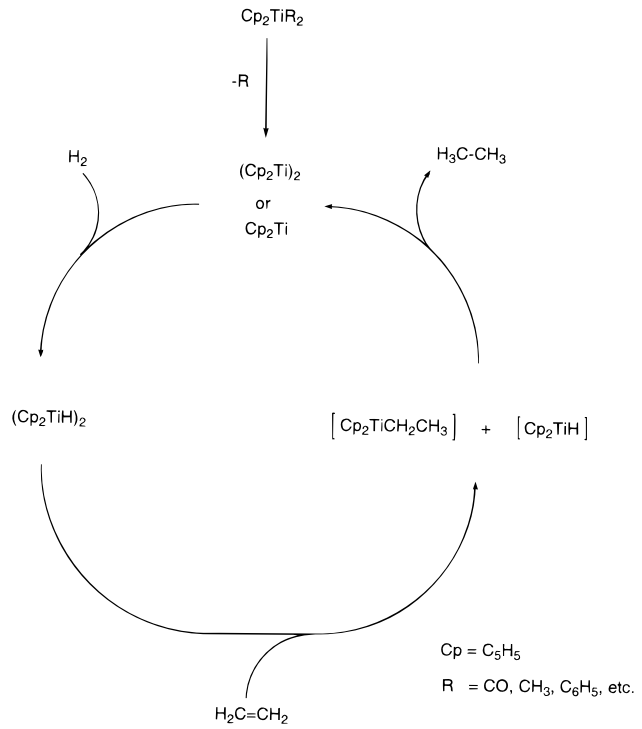

according to Scheme 1, but two types of reactions for the dimer formation can be considered: (i) through the dissociation of R group

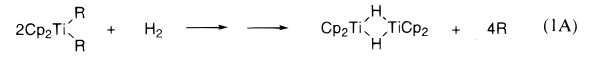

for R = CO, and (ii) through the formation of R−H

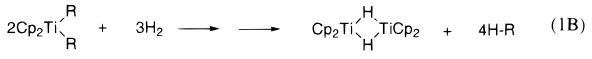

for R = CH_3, C_2H_5, η^3-C_5H_9, C_6H_5, etc. Since hydrogenation temperatures depend on a metallocene catalyst, the rate-determining step could be in reaction 1A or 1B. In other words, either reaction could present the highest activation barrier in the dimer formation, $(Cp_2TiH)_2$. In this study, we computed the possible transition states for the dimer formation reactions (1A or 1B) mediated by four titanocene complexes, (1) $Cp_2Ti(CO)_2$, (2) $Cp_2Ti(CH_3)_2$, (3) $Cp_2Ti(C_6H_5)_2$, and (4) $Cp_2Ti(p-C_6H_4-CH_3)_2$. This was accomplished by performing large quantum mechanical calculations to investigate the relative stabilities of several transition states. Also, the thermodynamic roles of catalysts in the overall hydrogenation reaction process are discussed.

Computational Methods

Without the use of symmetry considerations, conventional ab initio theories such as the coupled cluster method using single and double substitutions from Hartree−Fock (HF) determinant (CCSD)[5] and the Möller−Plesset (MP) correlation energy correction by perturbation method[6] with all-electron basis set (e.g., double-ζ quality basis set) are limited to calculations for the ground and transition states of small organometallic complexes. Furthermore, neither MP2 nor HF calculations yielded the correct bond distances of some transition metal complexes.[7] In contrast, the density functional theory (DFT)[8] is a powerful tool for the study of organometallic compounds. Thus, we employed DFT methods to calculate the ground and transition states of the hydrogenation reactions mediated by titanocene complexes. Calculations were carried out using the program packages, Dmol (DFT)[9] and Gaussian94 (DFT)[10] on a Cray-C94A at KUMHO Supercomputing Center in Kwangju and on Silicon Graphics (R10000 × 8 CPU Power Onyx) workstations in our laboratories. The basis functions of titanocene complexes for the GAUSSIAN94 DFT calculations were taken from Wachters' basis[11] (14s 11p 6d/10s 8p 3d) for Ti and from Huzinaga's basis[12] for C and O (9s 5p/4s 2p) and H (4s/2s), where the shell scale factor of hydrogen atom is set to 1.20. We called this basis set AE1s (all-electron basis set 1 with scaled shell factor of the hydrogen atom). In these DFT calculations, Becke3LYP (or B3LYP) and Becke3PW91 (or B3PW91) hybrid methods were employed with the following basis functions:

(1) AE2 (AE1 augmented by polarization (d) functions on carbon (0.75) and oxygen(0.85) atoms)

AE2s (scale): shell scale factor of hydrogen atom = 1.20

AE2ns (nonscale): shell scale factor of hydrogen atom = 1.00.

(2) AE3 (AE2 augmented by polarization (p) functions on all hydrogen (1.0) atoms)

AE3s: shell scale factor of hydrogen atom = 1.20

AE3ns: shell scale factor of hydrogen atom = 1.00.

(3) AE3p (AE2 augmented by polarization (p) functions on partial number of hydrogen(1.0) atoms)

AE3ps: shell scale factor of hydrogen atom = 1.20

AE3pns: shell scale factor of hydrogen atom = 1.00.

The DMol options used here are nonfrozen core orbitals, the Becke gradient-corrected exchange[13] and Lee, Yang, and Parr (BLYP) functionals[14] with double numerical basis plus polarization functions (DNP). The medium grid (DMol default option) was used since improving the grid quality did not significantly change the energy values.[15]

All geometries, including those of the transition states, were optimized by calculating analytical gradients and numerical (or analytical) Hessians. Hessian eigen values have either all positive values

(5) (a) Cizek, J. *Adv. Chem. Phys.* **1969**, *14*, 35. (b) Purvis, G. D.; Bartlett, R. J. *J. Chem. Phys.* 1**982**, *76*, 1910. (c) Scuseria, G. E.; Schaefer, H. F., III. *J. Chem. Phys*. 1**989**, *90*, 3700.

(6) Möller, C.; Plesset, M. S. *Phys. Rev*. **1934**, *46*, 618.

(7) (a) Lüthi, H. P.; Ammeter, J. H.; Almlöf, J.; Faegri, K., Jr. *J. Chem. Phys.* **1982**, *77*, 2002. (b) Jonas, V.; Thiel, W. *J. Chem. Phys*. **1995**, *102*, 8474.

(8) (a) Hohenberg, H.; Kohn, W. *Phys. Rev. B* **1964**, *136*, 864. (b) Parr, R. G.; Yang, W. *Density-Functional Theory of Atoms and Molecules*; Oxford University: New York, 1989. (c) Ziegler, T. *Chem. Rev*. **1991**, *95*, 7401. (d) Labanowski, J. K.; Andzelm, J. W., Eds. *Density Functional Methods in Chemistry*; Springer-Verlag: New York, 1991. (e) Fan, L.; Harrison, D.; Woo, T. K.; Ziegler, T. *Organometallics* **1995**, *14*, 2018. (f) Laird, B. B.; Ross, R. B.; Ziegler, T., Eds. *Chemical Applications of Density Functional Theory*; ACS Symposium Series 629, American Chemical Society: Washington, DC, 1995. (g) The 1998 Nobel Prize in Chemistry. The Royal Swedish Academy of Sciences, Information Department: Stockholm, Sweden, 1998 (http://www.nobel.se/announcement-98/chemistry98.html).

(9) DMol, User Guide, Version 95.0/3.0.0, BIOSYM/Molecular Simulations: 1995.

(10) Frisch, M. J.; Trucks, G. W., Schlegel, H. B.; Gill, P. M. W.; Johnson, B. G.; Robb, M. A., Cheeseman, J. R.; Keith, T.; Petersson, G. A.; Montgomery, J. A.; Raghavachari, K.; Al-Laham, M. A.; Zakrzewski, V. G.; Ortiz, J. V.; Foresman, J. B.; Cioslowski, J.; Stefanov, B. B.; Nanayakkara, A.; Challacombe, M.; Peng, C. Y.; Ayala, P. Y.; Chen, W.; Wong, M. W.; Andres, J. L.; Replogle, E. S.; Gomperts, R.; Martin, R. L.; Fox, D. J.; Binkley, J. S.; Defrees, D. J.; Baker, J.; Stewart, J. P.; Head-Gordon, M.; Gonzalez, C.; Pople, J. A. *Gaussian 94*, revision D.3; Gaussian Inc.: Pittsburgh, PA, 1995.

(11) Wachters, A. J. H. *J. Chem. Phys.* **1970**, *52*, 1033.

(12) Huzinaga, S. *J. Chem. Phys.* **1965**, *42*, 1293.

(13) Becke, A. D. *J. Chem. Phys.* **1988**, *88*, 2547.

(14) Lee, C.; Yang, W.; Parr, R. G. *Phys. Rev. B* **1988**, *37*, 786.

(15) Total energy difference of Cp_2Ti (singlet) between medium and fine grids at the geometry optimized with medium grid was about 0.5 kcal/mol.

Table 1. Interatomic Distances (Å) and Bond Angles (deg) for $(\eta^5\text{-}C_5H_5)_2Ti(CO)_2$ Obtained by DFT Calculations and Experiment

	DFT			
basis set	BLYP DNP	B3LYP AE2s (AE2ns)	B3PW91 AE2s (AE2ns)	expt.[a]
Ti−Cl	2.410	2.369 (2.371)	2.335 (2.336)	2.328
Ti−C4	2.410	2.369 (2.371)	2.335 (2.336)	2.356
Ti−C2	2.420	2.391 (2.392)	2.358 (2.359)	2.368
Ti−C5	2.420	2.391 (2.392)	2.358 (2.359)	2.354
Ti−C3	2.428	2.404 (2.406)	2.374 (2.375)	2.336
Ti−C6	2.428	2.404 (2.406)	2.374 (2.375)	2.340
Ti−C7	2.060	2.035 (2.306)	2.015 (2.015)	2.030
Ti−cent1	2.089	2.061 (2.063)	2.025 (2.026)	2.032
Ti−cent2	2.089	2.061 (2.063)	2.025 (2.026)	2.018
C1−C2	1.447	1.435 (1.434)	1.433 (1.433)	1.44
C4−C5	1.447	1.435 (1.434)	1.433 (1.433)	1.43
C2−C3	1.431	1.420 (1.420)	1.417 (1.417)	1.32
C5−C6	1.431	1.420 (1.420)	1.417 (1.417)	1.39
C3−C3′	1.437	1.426 (1.426)	1.424 (1.423)	1.38
C6−C6′	1.437	1.426 (1.426)	1.424 (1.423)	1.41
C7−O	1.181	1.166 (1.165)	1.165 (1.164)	1.15
C1−H1	1.102	1.078 (1.084)	1.079 (1.084)	
C4−H4	1.102	1.078 (1.084)	1.079 (1.084)	
C2−H2	1.103	1.078 (1.084)	1.078 (1.084)	
C5−H5	1.103	1.078 (1.084)	1.078 (1.084)	
C3−H3	1.102	1.078 (1.085)	1.079 (1.085)	
C6−H6	1.102	1.078 (1.085)	1.079 (1.085)	
C2−C1−C2′	107.8	107.8 (107.8)	107.8 (107.8)	108
C5−C4−C5′	107.8	107.8 (107.8)	107.8 (107.8)	107
C3−C2−C1	107.7	107.8 (107.8)	107.7 (107.7)	105
C6−C5−C4	107.7	107.8 (107.8)	107.7 (107.7)	108
C3′−C3−C2	108.7	108.3 (108.3)	108.4 (108.4)	111
C6′−C6−C5	108.4	108.3 (108.3)	108.4 (108.4)	109
C7−Ti−cent1	104.0	104.0 (103.9)	103.7 (103.7)	104.1
C7−Ti−cent2	104.0	104.0 (103.9)	103.7 (103.7)	105.4
cent1−Ti−cent2	140.7	140.7 (140.6)	141.6 (141.6)	138.6
C7−Ti−C7′	88.0	88.4 (88.4)	87.8 (87.8)	87.9
O−C7−Ti	179.0	179.8 (179.8)	179.3 (179.3)	179.4

[a] Reference 17.

(ground state) or only one negative value (transition state). We also confirmed that the ground-state geometries had all positive vibrational frequencies and that the transition-state geometries had one and only one imaginary frequency. The transition states were first optimized by the BLYP calculations. Here, at a fixed bond length (= *r*) between one of the H atoms of H_2 and the α-carbon atom of the Ti−R(R = CH_3, C_6H_6, or $C_6H_5CH_3$) bond to form R−H bond, say r = 1.70 Å, other internal coordinates were optimized. Then, r was reduced by 0.02 Å where other internal coordinates were again optimized. This procedure was repeated until the gradient of the H−C_α bond became less than 0.01 au (atomic unit = hartree). All internal coordinates were then completely optimized under the transition-state constraint. Transition-state calculations at the hybrid DFT levels were started at the BLYP optimum geometries and were continued until absolute values of the first derivatives of the total energy with respect to Cartesian coordinates reached less than 0.01 au or the rms forces were less than 0.002 au. The analytical Hessians were then computed, sometimes repeatedly, to obtain the real transition states. The hybrid calculations, B3LYP and B3PW91, of the transition states for $[Cp_2Ti(CH_3)_2\ (H_2)]$, $[Cp_2Ti(C_6H_5)_2\ (H_2)]$, and $[Cp_2Ti(C_6H_4{-}CH_3)_2\ (H_2)]$ with the AE3pns basis set with C_1 symmetry, that is, no symmetry, had 245, 429, and 467 contracted basis functions, respectively, and the calculations for the last two complexes took a large amount of CPU time to compute the analytical Hessians. Here, only hydrogens of the H_2 molecule were augmented by p-functions. Typically, the transition states were obtained within several geometry-optimization cycles after the calculations of the analytical Hessians. To investigate the possible reaction path for the hydrogenation reaction catalyzed by $Cp_2Ti(CH_3)_2$, we employed the intrinsic reaction coordinate (IRC) method,[16] which computes the path from the transition state to each of the minima. In addition, zero-point corrected energy (E_0), enthalpy (H), entropy (S) and Gibbs free energy (G) were obtained by computing translational, rotational, and vibrational corrections to total energy (E). Relative thermodynamic (ΔH, ΔS and ΔG) and kinetic parameters ($\Delta H^{\ddagger}$, $\Delta S^{\ddagger}$ and $\Delta G^{\ddagger}$) in gas phase are calculated at 298.15 ° K and 1atm pressure unless the conditions are specified otherwise.

Results and Discussion

Comparison of Optimum Geometries with Experiments. Table 1 shows the optimum geometries of $Cp_2Ti(CO)_2$ complexes obtained by BLYP, B3LYP, and B3PW91 and the X-ray diffraction data (R value = 0.086).[17] The atomic numbering scheme for this complex is shown in Figure 1. All theoretical methods gave C_{2v} symmetry, whereas the experimental geometry[17] is slightly distorted from C_{2v} symmetry. The largest difference between the experimental and theoretical geometries is R(C_2−C_3) or R(C_2'−C_3') (0.11 Å for BLYP, and 0.10 Å for both B3LYP and B3PW91). The experimental bond length (= 1.32 Å) of R(C_2−C_3) or R(C_2'−C_3') seems to be significantly shorter than that(= 1.39 Å) of R(C_5−C_6) or R(C_5'−C_6'). Under exact C_{2v} symmetry, these four bond lengths should be identical. Our optimum bond lengths of R(C_2−C_3) = R(C_2'−C_3') (= 1.431, 1.420, and 1.417 Å, with the BLYP, B3LYP, and B3PW91 methods, respectively) are closer to the experimental bond length of R(C_5−C_6) or R(C_5'−C_6'). Except for R(C_2−C_3) and R(C_2'−C_3'), the geometry differences are 0.01−0.09 Å (bond lengths) and 0−3° (bond angles) between BLYP and the experiment, 0.00−0.07 Å (bond lengths) and 0−3° (bond angles) between B3LYP and the experiment, and 0.00−0.04 Å

(16) (a) Gonzalez, C.; Schlegel, H. B. *J. Chem. Phys.* **1989**, *90*, 2154. (b) Gonzalez, C.; Schlegel, H. B. *J. Phys. Chem.* **1990**, *94*, 5523.

(17) Atwood, J. L.; Stone, K. E.; Alt, H. G.; Hrneir, D. C.; Rausch, M. D. *J. Organomet. Chem.* **1977**, *132*, 367.

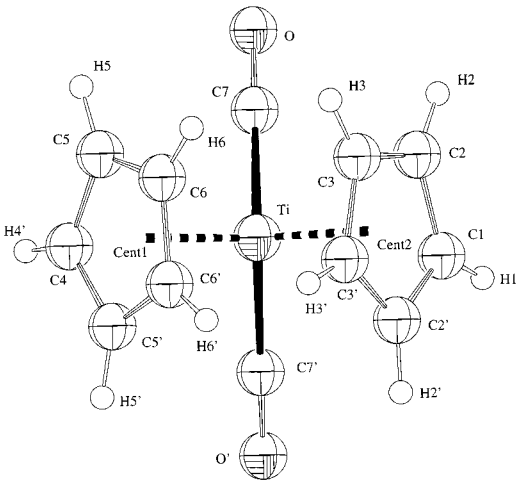

Figure 1. Structure of $(\eta^5\text{-}C_5H_5)_2Ti(CO)_2$.

Table 2. Bond Lengths (Å) and Bond Angles (deg) for Cp_2Ti Obtained by B3PW91/AE2ns

spin state symmetry	singlet C_s	triplet C_1
R(cent−Ti)	1.955	2.047
R_1'(C−C)	1.444	1.429
R_1(C−C)	1.448	1.426
R_2'(C−C)	1.424	1.426
R_3(C−C)	1.415	1.421
r_1(C−H)	1.085	1.086
r_2(C−H)	1.085	1.086
r_2(C−H)	1.085	1.086
r_3(C−H)	1.087	1.086
r_3'(C−H)	1.087	1.086
θ(cent1−Ti−cent2)	167.4	179.4
θ_1(C−C−C)	107.3	107.8
θ_2(C−C−C)	107.8	107.8
θ_2'(C−C−C)	107.5	108.1
θ_3(C−C−C)	108.8	108.1
θ_3'(C−C−C)	108.6	108.2
τ(HCCH)	0	−6.3

(bond lengths) and 0−3° (bond angles) between B3PW91 and the experiment. Therefore, the B3PW91 method with AE2 basis set yielded better results than the B3LYP or BLYP method. The optimum geometries of Cp_2Ti (singlet and triplet spin states) obtained by B3PW91/AE2ns are listed in Table 2. Singlet Cp_2Ti had C_s symmetry. Triplet Cp_2Ti showed no symmetry, but it was close to the structure slightly twisted from D_{5h} symmetry along the Cent−Cent′ axis.

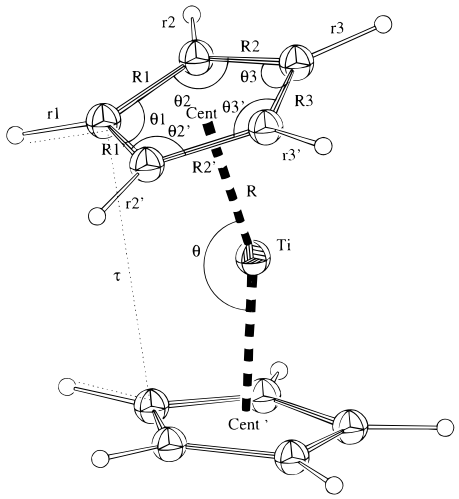

Although there is no experimental geometry available, Ziegler and co-workers[18] predicted θ (∠Cent−Ti−Cent′) to be 180° with C_{2v} symmetry for both singlet and triplet states. Our θ values for singlet and triplet Cp_2Ti are 167.4° and 179.4°, respectively, as shown in Table 2. Unless specified in the following sections, we have shown the results obtained by B3PW91 calculations with two kinds of basis functions, one with AE2ns basis set and another with AE3pns. The former basis set was used when hydrogen atoms were not directly bonded to the Ti atom, whereas the latter basis set was used when hydrogen atoms were directly bonded to Ti.

Mechanistic Investigation. As we described earlier, the activation barriers to the formation of a dimer complex, $(Cp_2TiH)_2$, could play a critical role in determining the hydrogenation temperature. Among four complexes, $Cp_2Ti(CO)_2$, $Cp_2Ti(CH_3)_2$, $Cp_2Ti(C_6H_5)_2$, and $Cp_2Ti(C_6H_4{-}CH_3)_2$, only $Cp_2Ti(CO)_2$ obeys the EAN (effective atomic number) rule so that $Cp_2Ti(CO)_2$ would form $(Cp_2TiH)_2$ differently compared with the others.

(a) $Cp_2Ti(CO)_2$ Catalyst. One of the Ti−C(Carbonyl) bonds of $Cp_2Ti(CO)_2$ is likely to be broken first because no more additional ligands are allowed for bonding to Ti,

$$Cp_2Ti(CO)_2 \rightarrow Cp_2Ti(CO) + CO \qquad \Delta G_{2A} \quad (2A)$$

Since titanocene (Cp_2Ti) exists in either singlet or triplet spin state, $Cp_2Ti(CO)$ could be further decomposed to the following products:

$$Cp_2Ti(CO)_2 \rightarrow Cp_2Ti\ (\text{singlet}) + CO \qquad \Delta G_s \quad (2B)$$

$$Cp_2Ti(CO)_2 \rightarrow Cp_2Ti\ (\text{triplet}) + CO \qquad \Delta G_t \quad (2C)$$

As shown in Table 3, the decomposition energy of $Cp_2Ti(CO)$ to the triplet state, or the total energy difference for reaction 2C ($= \Delta E_t$), is more favorable than the decomposition energy to the singlet state($= \Delta E_s$) by 9.1 kcal/mol (BLYP), 12.9 and 13.2 kcal/mol (B3LYP with AE2s and AE2ns), 13.4 and 13.6 kcal/mol (B3PW91 with AE2s and AE2ns), respectively. Although these values are lower than the previously reported value (16.7 kcal/mol),[18] it appears that reaction 2B proceeds much more slowly than reaction 2C.

Table 4 shows Ti−CO bond dissociation energies (ΔE_{2A}, ΔE_s, and ΔE_t), enthalpies (ΔH_{2A}, ΔH_s and ΔH_t), entropies ((ΔS_{2A}, ΔS_s, and ΔS_t) and Gibbs free energies (ΔG_{2A}, ΔG_s, and ΔG_t) for reactions 2A, 2B, and 2C, respectively, according to B3PW91/AE2ns calculations. For reactions 2A, 2B, and 2C, the ΔH values are a few kcal/mol less than the corresponding ΔE values. The difference between ΔH and ΔE, ($\Delta H - \Delta E$), is mostly a result of the contribution of zero-point vibrational energies ($= \Delta E_0 - \Delta E$). Also, entropy contributions ($= T\Delta S$) among these three reactions are similar (12−13 kcal/mol). As a result, the respective ΔG values for reactions 2A, 2B, and 2C (18.4, 26.9 and 12.8 kcal/mol) are equally (14−15 kcal/mol) less than the corresponding ΔE values (32.8, 41.4, and 27.7 kcal/mol). Experimentally, the possibility of $Cp_2Ti(\text{triplet}){-}Cp_2TiTiCp_2$ equilibrium[4] was indicated from magnetic susceptibility measurements. However, computed values of ΔE from both BLYP/DNP and B3PW91/AE2ns showed that the dimer, $Cp_2Ti{-}TiCp_2$, did not get any energy gain compared with the monomer form, Cp_2Ti. In other word, there was no appreciable bonding between two Ti atoms in the dimer, $Cp_2Ti{-}TiCp_2$.

(18) Harrod, J. F.; Ziegler, T.; Tschinke, V. *Organometallics* **1990**, *9*, 897.

Table 3. Total Energies (Hartrees) of $Cp_2Ti(CO)_2$, $Cp_2Ti(CO)$, Cp_2Ti, and CO and Bond Dissociation Energies (kcal/mol) of $Cp_2Ti(CO)_2$

	BLYP	B3LYP		B3PW91	
method basis set	DNP	A2s	A2ns	A2s	A2ns
total energies					
$Cp_2Ti(CO)_2$	−1463.2811	−1463.3607	−1463.3605	−1463.0836	−1463.0849
$Cp_2Ti(CO)$	−1349.8929	−1349.9838	−1349.9835	−1349.7517	−1349.7528
$Cp_2Ti(S)$	−1236.4910	−1236.5939	−1236.5936	−1236.4059	−1236.4071
$Cp_2Ti(T)$	−1236.5055	−1236.6144	−1236.6145	−1236.4273	−1236.4288
CO	−113.3369	−113.3287		−113.2798	
bond dissociation energies					
ΔE_{2A}[a]	32.2	30.3	32.7	30.3	32.8
ΔE_s[b]	40.8	38.4	38.4	41.4	41.4
ΔE_t[c]	31.6	25.5	25.2	28.0	27.8
ΔE_{st}[d]	9.1	12.9	13.2	13.4	13.6

[a] Total energy change in reaction 2A. [b] Total energy change in reaction 2B. [c] Total energy change in reaction 2C. [d] Energy difference between singlet and triplet Cp_2Ti. Positive sign means that the triplet Cp_2Ti is more stable than the singlet Cp_2Ti.

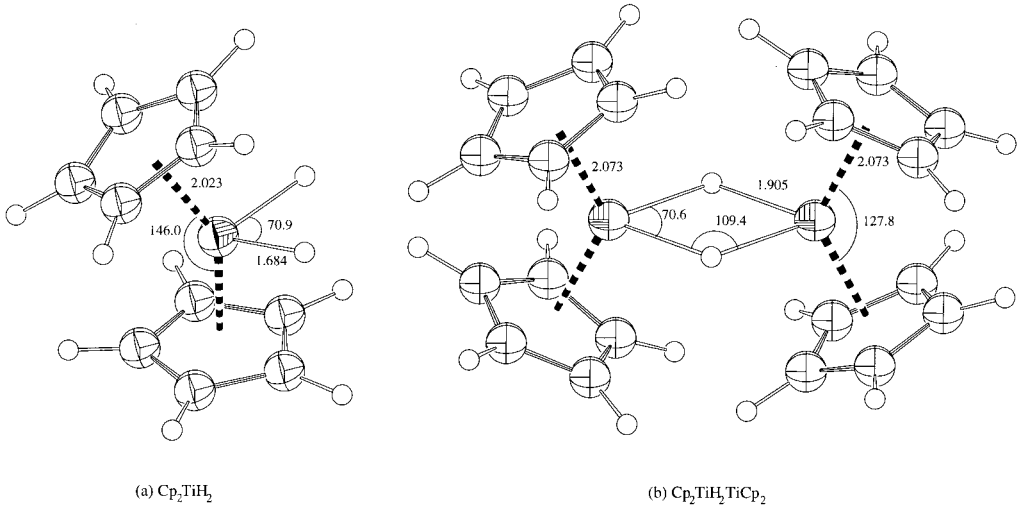

Figure 2. B3PW91-computed bond lengths (Å) and bond angles (deg) of (a) Cp_2TiH_2 and (b) $(Cp_2TiH)_2$.

Table 4. B3PW91-Computed Bond Dissociations (kcal/mol) in Reactions 2A, 2B, and 2C ($Cp_2Ti(CO)_2$ Catalyst)

	reaction 2A	reaction 2B	reaction 2B
ΔE	32.8	41.4	27.8
ΔE_0	30.0	37.9	24.8
ΔH	30.9	38.9	25.8
$T\Delta S$	12.5	12.0	13.0
ΔG	18.4	26.9	12.8

Once the Cp_2Ti (triplet) is formed, it can react with hydrogen, followed by the formation of a dimer complex, $(Cp_2TiH)_2$

$$Cp_2Ti\ (triplet) + H_2 \rightarrow Cp_2TiH_2 \qquad \Delta G_{3A} \qquad (3A)$$

$$Cp_2Ti\ (triplet) + Cp_2TiH_2 \rightarrow Cp_2TiH_2TiCp_2 \qquad \Delta G_{3B} \qquad (3B)$$

Some of the important geometries of Cp_2TiH_2 and $(Cp_2TiH)_2$ are shown in Figure 2. The former has C_{2v} symmetry and the latter is nearly D_2 in symmetry. The ΔH values are −4.0 kcal/mol and +4.6 kcal/mol for reaction 3A and 3B, respectively. Both ΔHs are larger by a few kcal/mol than the corresponding ΔE values, in contrast with reactions 2A, 2B, and 2C. Also, ΔGs for reactions 3A and 3B (+7.4 and +22.9 kcal/mol, respectively) are larger than the respective ΔH's. This is because of the negative contributions of the entropy terms. Note that in the similar reaction

$$[C_5(CH_3)_5]_2Ti\ (triplet) + H_2 \rightarrow [C_5(CH_3)_5]_2TiH_2 \qquad (3A)'$$

the enthalpy change in solution, ΔH, was estimated to be −12 ± 2 kcal/mol.[4] Finally, ethene is hydrogenated by $(Cp_2TiH)_2$,

$$Cp_2TiH_2TiCp_2 + H_2C{=}CH_2 \rightarrow 2Cp_2Ti\ (triplet) + H_3C{-}CH_3 \qquad \Delta G_{3C}. \qquad (3C)$$

The ΔH_{3C} and ΔG_{3C} are −38.1 and −59.4 kcal/mol, respectively. Since reaction 3B is nonspontaneous at room temperature, the dimer $(Cp_2TiH)_2$ would not form without heating. Instead of reactions 3B and 3C, Cp_2TiH_2 would directly hydrogenate,

$$Cp_2TiH_2 + H_2C{=}CH_2 \rightarrow 2Cp_2Ti\ (triplet) + H_3C{-}CH_3 \qquad \Delta G_{3D}. \qquad (3D)$$

The ΔH_{3D} and ΔG_{3D} are −33.5 kcal/mol and −36.4 kcal/mol, respectively. Therefore, a possible reaction order of the ethene hydrogenation catalyzed by $Cp_2Ti(CO)_2$ at room temperature would be reaction 2A → 2C → 3A → 3D as shown in Figure 3. Among reactions 2A, 2C, and 3A, reaction 2A is the rate-determining step, where $\Delta G_{2A} = \Delta H_{2A} - T\Delta S_{2A} = 30.9 - 12.5 = 18.4$ kcal/mol at room temperature. Since ΔS_{2A} is positive, ΔG_{2A} would be smaller than 18.4 kcal/mol at higher temperature, whereas ΔG_{2A} would be larger at lower temperature. This is based on the fact that, in general, ΔH and ΔS change much more slowly than the temperature (or ΔG) changes. In fact, at 0°K, $\Delta G_{2A} = \Delta E_{2A0} = 30.0$ kcal/mol, which is close to $\Delta H_{2A} = 30.9$ kcal/mol. Furthermore, second Ti−C(CO) bond dissociation(reaction 2C) and the formation of Cp_2-

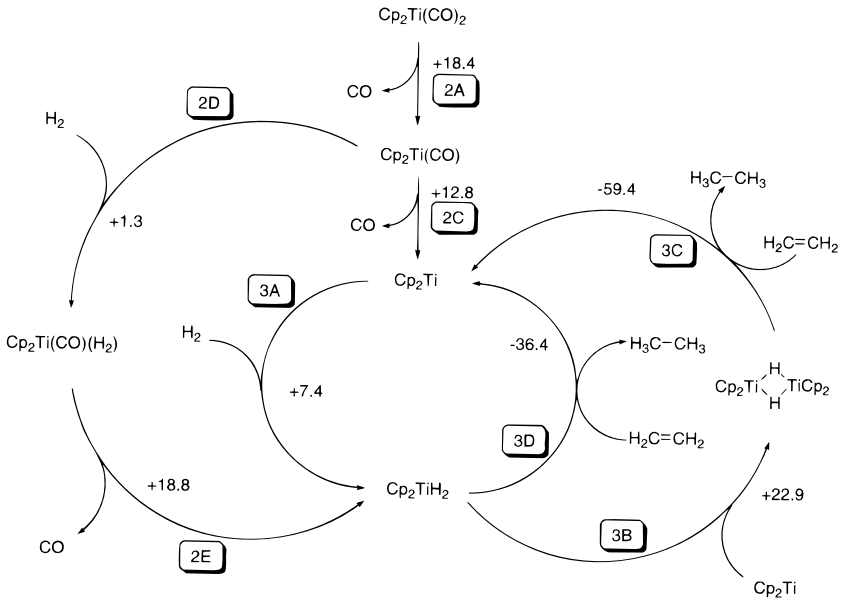

Figure 3. Gibbs free-energy changes (kcal/mol) from bond dissociations of $Cp_2Ti(CO)_2$ to hydrogenation of $H_2C{=}CH_2$ computed by B3PW91.

TiH_2 (reaction 3A) take place nonspontaneously (ΔG = 12.8 and 7.4 kcal/mol, respectively). Also, the activation barrier for reaction 3D must be overcome for ethene hydrogenation to occur. So, continuous heating is necessary until the Ti−C(CO) bond dissociations (reactions 2A and 2C) and the activation barriers (reactions 3A and 3D) are overcome. Experimentally, $Cp_2Ti(CO)_2$-catalyzed ethene hydrogenation occurs at 65 °C.[4] When the temperature is decreased from 298 K to 0 K, ΔG_{3B} decreases from 23 kcal/mol to 5 kcal/mol because of the negative entropy term. On the other hand, ΔG_{3B} would be larger than 23 kcal/mol above room temperature so that reaction 3B would occur much more slowly than reaction 2A.

Triplet Cp_2Ti produced in reaction 3D is recycled in reaction 3A. Note that the sum of reactions 3A and 3D (or reactions 3A, 3B, and 3C) is the net hydrogenation of $H_2C{=}CH_2$,

$$H_2 + H_2C{=}CH_2 \rightarrow H_3C{-}CH_3 \qquad \Delta G_{3S}. \qquad (3S)$$

The ΔH_{3S}, $T\Delta S_{3S}$ and ΔG_{3S} are, respectively, −37.5, −8.4, and −29.1 kcal/mol, which are in fair agreement with the experimental values (= −32.7, −8.6, and −24.1 kcal/mol, respectively).[19] From the above results, the $Cp_2Ti(CO)_2$-catalyzed hydrogenation reaction should proceed in the order

$$2A \rightarrow 2C\ (\rightarrow 3A \rightarrow 3D)_n \qquad (O1)$$

where *n* means that reactions 3A and 3D repeat n times until the activity of Cp_2Ti or Cp_2TiH_2 is terminated (also see Figure 3). Since reaction 3D takes place spontaneously (ΔG = −36.4kcal/mol), the excess Gibbs free energy can overcome reaction 3A (ΔG = +7.4 kcal/mol) and even reaction 3B (ΔG = +22.9 kcal/mol). Once reaction 3B proceeds, the hydrogenation of ethene occurs spontaneously (ΔG of reaction 3C = −59.4 kcal/mol). Therefore, another possible reaction order would be

$$2A \rightarrow 2C \rightarrow 3A \rightarrow 3D\ (\rightarrow 3A \rightarrow 3B \rightarrow 3C)_n \qquad (O2)$$

However, reactions 3B and 3C would take place much more slowly than reaction 3D. The experimental temperature (65 °C) is therefore interpreted as the target temperature to overcome the Ti−C(CO) bond dissociations (reactions 2A and 2C) and the activation barriers (reactions 3A and 3D). Heat produced or an excess Gibbs free energy available from reaction 3D would be sufficient to overcome reactions 3A and even 3B in the catalytic cycle. As the catalytic cycle proceeds, the temperature of the system increases without further heating. At 100 °C or higher temperature, the catalytic cycles are terminated since of $(Cp_2TiH)_2$ decomposes to $[(C_5H_5)(C_5H_4)TiH]_2$.[4]

There may be other possible reaction pathways. After $Cp_2Ti(CO)$ is formed in reaction 2A, it could react with hydrogen:

$$Cp_2Ti(CO) + H_2 \rightarrow 2Cp_2Ti\ (CO)(H_2) \qquad \Delta G_{2D} \qquad (2D)$$

followed by the Ti−C(CO) bond dissociation of $Cp_2Ti(CO)(H_2)$:

$$Cp_2Ti(CO)(H_2) \rightarrow Cp_2TiH_2 + CO \qquad \Delta G_{2E} \qquad (2E)$$

Here, two possible structures for $Cp_2Ti(CO)(H_2)$ are considered

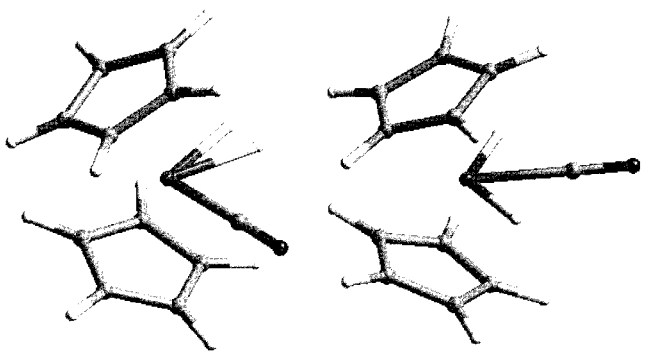

Structure I Structure II

Structure I, where Cp_2TiH_2 forms adducts with CO in the lateral position,[20] is more stable by 7.3 kcal/mol in enthalpy term than Structure II with the central coordination of CO in $Cp_2Ti(CO)(H_2)$. In structure I, the H−H bond distance is 0.847 Å, and the Ti−H bond lengths are 1.829 and 1.832 Å; titanium atom and

(19) Atkins, P. W. *Physical Chemistry*; Oxford University Press: Oxford, 1990.

(20) Marsella, J. A.; Curtis, C. J.; Bercaw, J. E.; Caulton, K. G. *J. Am. Chem. Soc.* **1980**, *102*, 7244.

carbonyl and dihydrogen groups are essentially in the same plane. Despite the theoretically predicted titanocene−dihydrogen complex,[21] a stable dihydrogen complex with group 4 metals has not yet been reported.[22] With structure I, the ΔH and ΔG are, respectively, −11.5 kcal/mol and +1.3 kcal/mol for reaction 2D, and +33.6 kcal/mol and +18.8 kcal/mol for reaction 2E. ΔG for reaction 2E is essentially the same large value as for reaction 2A. Therefore, the following pathways:

$$2A \rightarrow 2D \rightarrow 2E \rightarrow 3D\ (\rightarrow 3A \rightarrow 3D)_n \qquad (O3)$$

or

$$2A \rightarrow 2D \rightarrow 2E \rightarrow 3D\ (\rightarrow 3A \rightarrow 3B \rightarrow 3C)_n. \qquad (O4)$$

proceed much more slowly than the reaction orders, O1 and O2 (also see Figure 3).

(b) $Cp_2Ti(CH_3)_2$ Catalyst. Hydrogenolysis of $Cp_2Ti(CH_3)_2$ takes place at 0 °C,[4] whereas its decomposition occurs at 97 °C.[23] Other studies report that $Cp_2Ti(CH_3)_2$ decomposed even at room temperature rapidly in light and more slowly in the dark.[24,25] The decomposition of this complex would not directly dissociate to Cp_2Ti and CH_4, but it could proceed through hydrogen abstraction from the cyclopentadienyl rings,[26,27] from another R group,[26−28] or from solvents.[27] Therefore, some gases such as hydrogen or other effects might be involved, causing the hydrogenation reaction by $Cp_2Ti(CH_3)_2$ to occur at a much lower temperature than the decomposition temperature.

The hydrogenation by $Cp_2Ti(CH_3)_2$ could take place through so-called σ bond metathesis[29] for the Ti−C(CH_3) bond and H−H bond, as shown in the following two steps: first, the formation of $Cp_2Ti(H)(CH_3)$ through a four-center transition state composed of carbon, hydrogen, and titanium

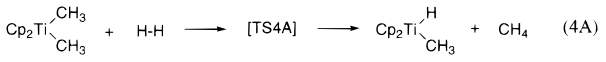

(4A)

and second, the formation of Cp_2TiH_2

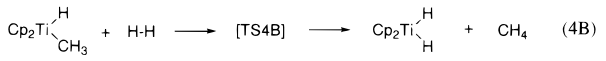

(4B)

The reductive elimination of methane to form Cp_2Ti may take place at the same time as reaction 4B

(4C)

followed by reaction 3A and reaction 3D or reactions 3B and 3C. Triplet Cp_2Ti produced in reaction 3C or 3D is recycled in reaction 3A, as described in the $Cp_2Ti(CO)_2$-catalysis reaction. The geometries of the transition states, TS4A, TS4B, and TS4C, are shown in Figure 4. Note that thermal decomposition of $Cp_2Ti(CH_3)_2$ yields primarily methane with only a trace of ethane.[26] The computed activation parameters and relative thermodynamic values for reactions 4A, 4B, and 4C are shown in Table 5 and Figure 5. It turned out that the Gibbs free energy of activation for reaction 4A ($\Delta G^{\ddagger} = 31.5$ kcal/mol) was higher than that for reaction 4B or 4C, depending on the pathway.

To elucidate theoretically the reaction path for reaction 4A, the IRC path-following calculations[16] were carried out by B3PW91/AE2S computations.[30] The results are shown in Figure 6. As a hydrogen molecule approaches $Cp_2Ti(CH_3)_2$ (Figure 6a), dihydrogen is elongated. At the same time, a hydrogen atom of H_2 approaches one of the methyl groups. At the transition state (Figure 6b), dihydrogen is more elongated. Also, there is more bonding character between a hydrogen atom of H_2 and one of the methyl groups. At the final point (Figure 6c), a hydrogen atom of H_2 forms almost a single bond with a methyl group to become an isolated methane while another hydrogen of H_2 bonds to the Ti metal. The formation of CH_4 from a similar reaction system ($Cl_2Ti(CH_3)_2 + H_2$) was also confirmed by density functional (VWN[31]) molecular dynamics and BLYP calculations, using the FastStructure Simulated Annealing module in insightII.[32]

Since the Gibbs free energy of activation for reaction 4A ($\Delta G^{\ddagger} = \Delta H^{\ddagger} - T\Delta S^{\ddagger} = 22.5 + 9.0 = 31.5$ kcal/mol) is the highest among reactions 4A, 4B, 4C, 3A, 3B, 3C, and 3D, reaction 4A is rate-determining at room temperature. Unlike first dissociation of Ti−CO bond for $Cp_2Ti(CO)_2$, $\Delta S^{\ddagger}$ for reaction 4A is negative, so $\Delta G^{\ddagger}$ for reaction 4A would be smaller than 31.5 kcal/mol at lower temperature. In fact, $\Delta G^{\ddagger}$ at 0 K will be equal to $\Delta E_0^{\ddagger} = 24.6$ kcal/mol. Also, ΔG for reaction 3B will be less than 22.9 kcal/mol at low temperature (at 0 K, $\Delta G = \Delta E_0 = 5.2$ kcal/mol) as described earlier. Thus, at lower than room temperature, $Cp_2Ti(CH_3)_2$-catalyzed hydrogenation could take place in the order

$$4A \rightarrow 4C\ (\rightarrow 3A \rightarrow 3D)_n$$

$$4A \rightarrow 4B \rightarrow 3D\ (\rightarrow 3A \rightarrow 3D)_n$$

$$4A \rightarrow 4C\ (\rightarrow 3A \rightarrow 3B \rightarrow 3C)_n$$

or

$$4A \rightarrow 4B \rightarrow 3B \rightarrow 3C\ (\rightarrow 3A \rightarrow 3B \rightarrow 3C)_n$$

Near 0 K, however, limited collisions between particles are possible so that not much ethene hydrogenation would take place. Therefore, the $Cp_2Ti(CH_3)_2$-catalyzed hydrogenation temperature (0 °C) is interpreted as the temperature needed to overcome the activation barrier of the rate-determining step (reaction 4A). The excess Gibbs free energy ($\Delta G = -21.2$ kcal/mol) available from reaction 4A can overcome the activation barrier of reaction 4B ($\Delta G^{\ddagger} = 19.1$ kcal/mol) or reaction 4C ($\Delta G^{\ddagger} = 13.4$ kcal/mol). Furthermore, Gibbs free energy available from reaction 4C ($\Delta G = -25.1$ kcal/mol) is sufficient

(21) Margl, P. M.; Woo, T. K.; Blochl, P. E.; Ziegler, T. *J. Am. Chem. Soc.* **1998**, *120*, 2174.
(22) (a) Lin, Z.; Hall, M. B. *Coord. Chem. Rev.* **1994**, *135/136*, 845. (b) Basch, H.; Musaev, D. G.; Morokuma, K.; Fryzuk, M. D.; Love, J. B.; Seidel, W. W.; Albinati, A.; Koetzle, T. F.; Klooster, W. T.; Mason, S. A.; Eckert, J. *J. Am. Chem. Soc.* **1999**, *121*, 523.
(23) Cardin, D. J. In *Dictionary of Organometallic Compounds*; Buckingham, J., Ed.; Chapman and Hall: London, 1984; Vol. 2, p 2245.
(24) Piper, T. S.; Wilkinson, G. J. *Inorg. Nucl. Chem.* **1956**, *3*, 104.
(25) Clauss, K.; Bestian, H. *Liebigs Ann. Chem.* **1962**, *654*, 8.
(26) Erskine, G. J.; Wilson, D. A.; McCowan, J. D. *J. Organomet. Chem.* **1976**, *114*, 119.
(27) Boekel, C. P.; Teuben, J. H.; de Liefde Meijer, H. J. *J. Organomet. Chem.* **1974**, *81*, 371.
(28) McDade, C.; Green, J. C.; Bercaw, J. E. *Organometallics* **1982**, *1*, 1629.
(29) (a) Bruno, J. W.; Marks, T. J.; Day, V. W. *J. Am. Chem. Soc.* **1982**, *104*, 7357. (b) Watson, P. L. *J. Am. Chem. Soc.* **1983**, *105*, 6491. (c) Thompson, M. E.; Baxter, S. M.; Bulls, A. R.; Burger, B. J., Nolan, M. C.; Santarsiero, B. D., Schaefer W. P., Bercaw, J. E. *J. Am. Chem. Soc.* **1987**, *109*, 203. (d) Woo, H.-G.; Walzer, J. F.; Tilley, T. D. *J. Am. Chem. Soc.* **1992**, *114*, 7047. (e) Ziegler, T.; Floga, E.; Berces, A. *J. Am. Chem. Soc.* **1993**, *115*, 636.
(30) B3PW91/AE2s calculations of the barrier height for reaction 4A are very similar to B3PW91/AE3pns calculations, and yet the former calculations take less computation time.
(31) Vosko, S. H.; Wilk, L.; Nusair, M. *Can. J. Phys.* **1980**, *58*, 1200.
(32) InsightII, User Guide, Version 95.0/3.0.0, BIOSYM/Molecular Simmulations, 1995.

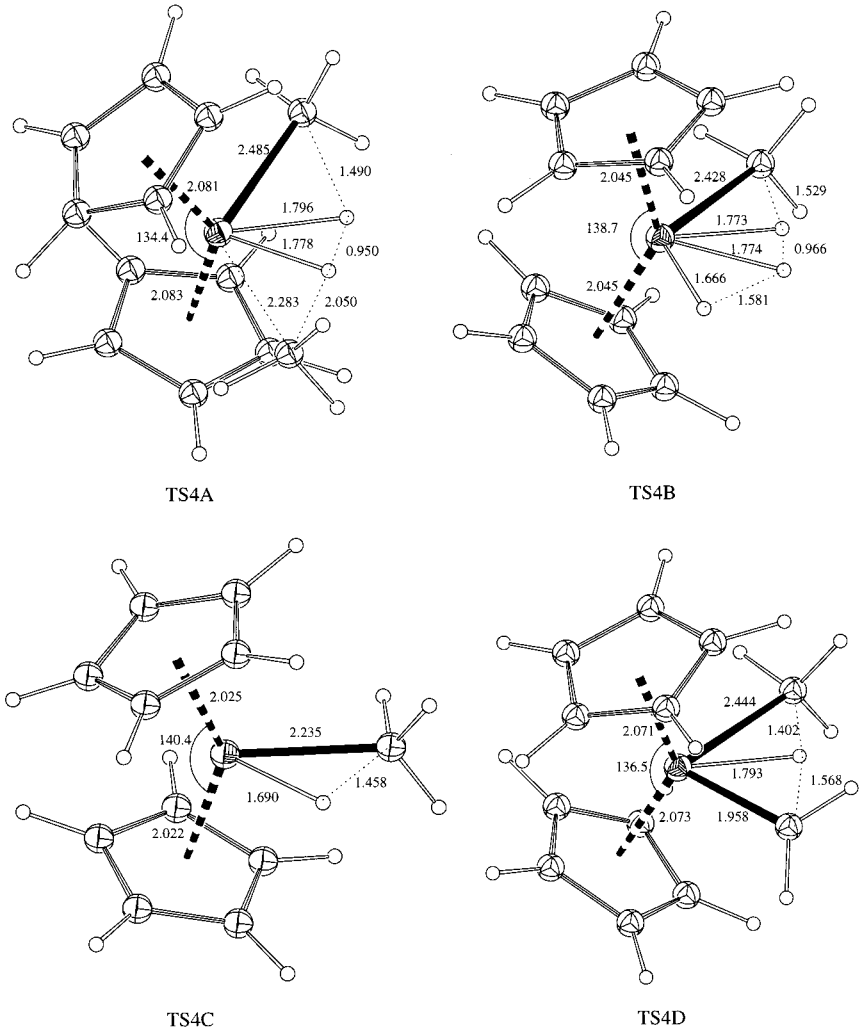

Figure 4. B3PW91-computed optimum geometries of transition states in reactions, 4A, 4B, 4C, and 4D ($Cp_2Ti(CO)_2$ catalyst).

Table 5. B3PW91-Computed Activation Parameters and Relative Thermodynamic Values (kcal/mol) in Reactions 4A, 4B, and 4C ($Cp_2Ti(CH_3)_2$ Catalyst)

(1) reaction 4A	$Cp_2Ti(CH_3)_2 + H_2$	$[Cp_2Ti(CH_3)_2(H_2)]^‡$	$Cp_2Ti(H)(CH_3) + CH_4$
ΔE	0	+20.2	−18.4
ΔE_0	0	+24.6	−15.5
ΔH	0	+22.5	−16.1
$T\Delta S$	0	−9.0	+5.1
ΔG	0	+31.5	−21.2
(2) reaction 4B	$Cp_2Ti(H)(CH_3) + H_2$	$[Cp_2Ti(H)(CH_3)_2(H_2)]^‡$	$Cp_2TiH_2 + CH_4$
ΔE	0	+5.9	−17.8
ΔE_0	0	+10.9	−14.3
ΔH	0	+8.4	−15.2
$T\Delta S$	0	−10.7	+2.5
ΔG	0	+19.1	−17.7
(3) reaction 4C	$Cp_2Ti(H)(CH_3)$	$[Cp_2Ti(H)(CH_3)]^‡$	$Cp_2Ti + CH_4$
ΔE	0	+13.3	−12.1
ΔE_0	0	+13.1	−12.3
ΔH	0	+12.7	−11.2
$T\Delta S$	0	−0.7	+13.9
ΔG	0	+13.4	−25.1

to overcome the activation Gibbs free energy for reaction 3A. A large amount of heat is produced in reaction 3D or 3C so that the temperature of the system goes up during catalytic cycles. The catalytic cycles are, however, terminated at 100 °C or higher temperatures as described earlier.

An alternative mechanism is possible through α-H abstraction or α-H elimination to form $Cp_2Ti{=}CH_2$,[28]

$$Cp_2Ti(CH_3)_2 \longrightarrow [TS4D] \longrightarrow Cp_2Ti{=}CH_2 + CH_4 \qquad (4D)$$

And then,

$$Cp_2Ti{=}CH_2 + H_2 \rightarrow Cp_2TiH(CH_3) \qquad (4E)$$

followed by the σ bond metathesis reaction,

$$Cp_2Ti(H)(CH_3) + H\text{-}H \longrightarrow [TS4B] \longrightarrow Cp_2Ti(H)_2 + CH_4 \qquad (4B)$$

or

$$Cp_2Ti{=}CH_2 \rightarrow Cp_2Ti + CH_2 \qquad (4F)$$

The reductive elimination of methane to form Cp_2Ti, that is, reaction 4C, may take place at the same time as reaction 4B. The geometry of the transition state, TS4D, is also shown in Figure 4. The activation Gibbs free energies ($\Delta G^‡$s) for reactions 4D, 4B, 4C, and 4F are 30.3, 19.1, 13.4, and 54.4 kcal/mol, respectively. The ΔH and ΔG for reaction 4E are −28.8 and −21.5 kcal/mol, respectively. Apparently, a direct dissociation

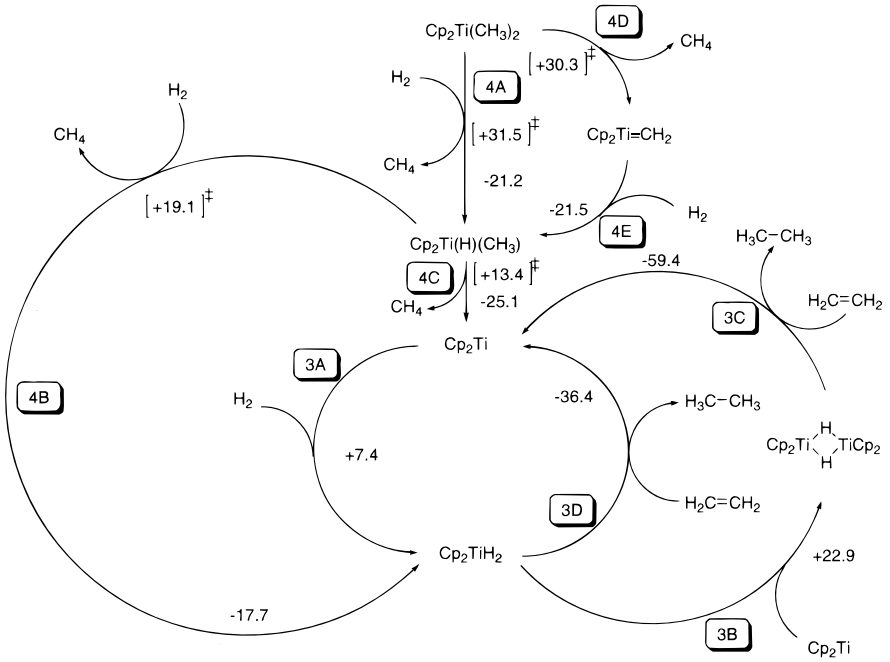

Figure 5. Gibbs free-energy changes (kcal/mol) for reactions, 4A, 4B, 4C, 3A, 3B, 3C, and 3D computed by B3PW91. Values in [ ]‡ are Gibbs free energies of activation for corresponding reactions.

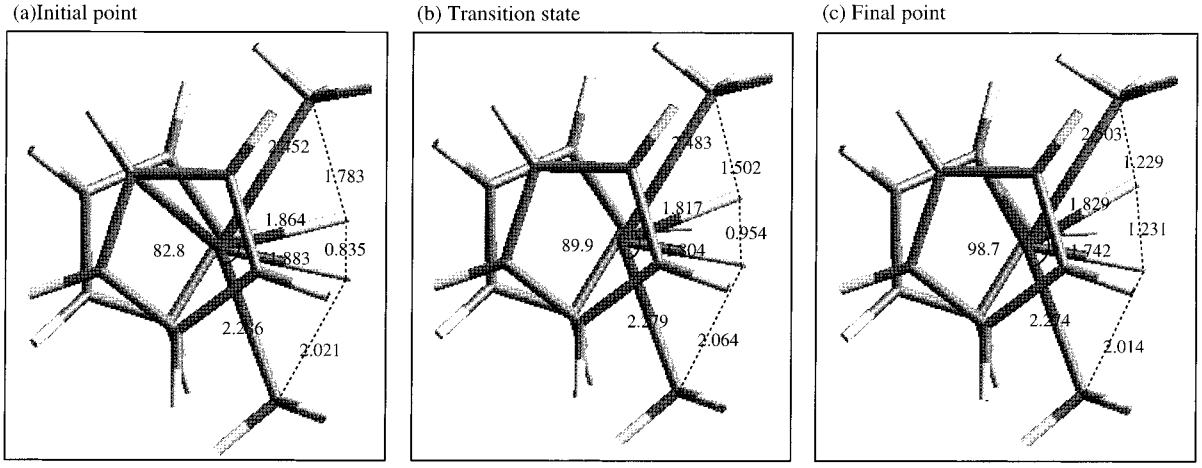

Figure 6. IRC path following in reaction 4A: (a) initial point, (b) transition state, and (c) final point.

reaction of Ti═C bond (reaction 4F) is not likely. When reactions 4D, 4E, 4B, 4C, and 3A take place, reaction 4D has the highest Gibbs free energy of activation, which is comparable to the previous σ bond metathesis reaction (Gibbs free energy of activation for reaction 4A = 31.5 kcal/mol). The activation parameters at room temperature for reaction 4D are $\Delta H^{\ddagger} = 29.5$ kcal/mol and $T\Delta S^{\ddagger} = -0.8$ kcal/mol, whereas those for reaction 4A are $\Delta H^{\ddagger} = 22.5$ kcal/mol and $T\Delta S^{\ddagger} = -9.0$ kcal/mol. Since $\Delta S^{\ddagger}$ for reaction 4D is very small, $\Delta G^{\ddagger}$ would be close to $\Delta H^{\ddagger}$. For example, at 0 K, $\Delta G^{\ddagger} = \Delta E_0^{\ddagger} = 29.9$ kcal/mol $\approx \Delta H^{\ddagger}$. Experimentally, $\Delta G^{\ddagger} = \Delta H^{\ddagger} - T\Delta S^{\ddagger} = 27.6 - 371.15 \times (-0.00285) = 28.8$ kcal/mol for the thermal decomposition of $(\eta^5\text{-}C_5Me_5)_2Ti(CH_3)_2$ at 98 °C.[28] Simple linear extrapolation of $\Delta G^{\ddagger}$ for reaction 4D at 98 °C is about 30−31 kcal/mol, which is close to $\Delta G^{\ddagger}$ for the thermal decomposition of $(\eta^5\text{-}C_5Me_5)_2$-Ti $(CH_3)_2$. These activation parameters are close to our computed values for reaction 4D. Thus, the following reactions could also occur:

$$4D \rightarrow 4E \rightarrow 4B \text{ (or } 4C \rightarrow 3A) \rightarrow 3D \ (\rightarrow 3A \rightarrow 3D)_n$$

or

$$4D \rightarrow 4E \rightarrow 4B \text{ (or } 4C \rightarrow 3A) \rightarrow 3D \ (\rightarrow 3A \rightarrow 3B \rightarrow 3C)_n$$

Since the decomposition of $Cp_2Ti(CH_3)_2$ through the α-H abstraction (reaction 4D) has a small entropy change, reaction 4D proceeds more rapidly at high temperatures, which is contrary to the case of the first σ bond metathesis (reaction 4A). From these results, an ethene hydrogenation reaction catalyzed by $Cp_2Ti(CH_3)_2$ would take place through α-H abstraction (reaction 4D) above room temperature; however, it would occur through σ bond metathesis (reaction 4A) at a lower temperature.

Industrially, the hydrogenations of unsaturated double bonds of the diene units on conjugated diene polymers and copolymers (such as polybutadiene, polyisoprene, and styrene−butadiene−styrene block copolymer) catalyzed by $Cp_2Ti(CH_3)_2$ are generally carried out in the range of −20 to 150 °C, or preferably in the range of 20 to 80 °C.[3a] This is because at lower than −20 °C, (i) the catalyst activity is reduced (ii) hydrogenation speed is slow, and (iii) a large amount of catalyst is needed, and at

Table 6. B3PW91-Computed Activation Parameters and Relative Thermodynamic Values (kcal/mol) in Reactions 5A, 5B, and 5C ($Cp_2Ti(C_6H_5)_2$ Catalyst)

(1) reaction 5A	$Cp_2Ti(C_6H_5)_2 + H_2$	$[Cp_2Ti(C_6H_5)_2(H_2)]^‡$	$Cp_2Ti(H)(C_6H_5) + C_6H_6$
ΔE	0	+21.5	−19.6
ΔE_0	0	+25.1	−16.0
ΔH	0	+23.2	−17.6
$T\Delta S$	0	−8.8	+5.5
ΔG	0	+32.0	−23.1

(2) reaction 5B	$Cp_2Ti(H)(C_6H_5) + H_2$	$[Cp_2Ti(H)(C_6H_5)_2(H_2)]^‡$	$Cp_2TiH_2 + C_6H_6$
ΔE	0	+9.8	−13.9
ΔE_0	0	+13.9	−9.9
ΔH	0	+11.6	−11.8
$T\Delta S$	0	−10.7	+3.2
ΔG	0	+22.3	−15.0

(3) reaction 5C	$Cp_2Ti(H)(C_6H_5)$	$[Cp_2Ti(H)(C_6H_5)]^‡$	$Cp_2Ti + C_6H_6$
ΔE	0	+13.5	−8.2
ΔE_0	0	+13.1	−7.9
ΔH	0	+12.7	−7.7
$T\Delta S$	0	−1.8	+14.6
ΔG	0	+14.5	−22.3

higher than 150 °C, (iv) the catalyst is inactivated, (v) the polymer is decomposed or gelled, and (vi) the hydrogenation tends to occur additionally on the aromatic portion of the polymer.

(c) $Cp_2Ti(C_6H_5)_2$ and $Cp_2Ti(C_6H_4CH_3)_2$ Catalysts. We assume that hydrogenation reactions by $Cp_2Ti(C_6H_5)_2$ and $Cp_2Ti(C_6H_4CH_3)_2$ could also proceed via the σ bond metathesis reactions,

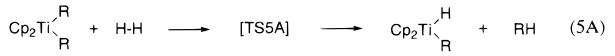

Here R = $-C_6H_5$ or $-C_6H_4CH_3$. Then, the formation of Cp_2TiH_2,

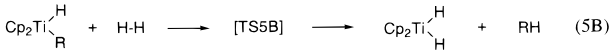

In addition to reaction 5B, the reductive elimination of RH to form Cp_2Ti may take place at the same time,

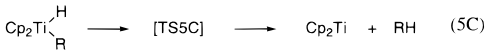

followed by reaction 3A and reaction 3D or reactions 3B and 3C, as described in the section on $Cp_2Ti(CH_3)_2$ catalyst. The activation parameters and the relative thermodynamic values for reactions 5A, 5B, and 5C with R = $-C_6H_5$ are listed in Table 6 and Figure 7. The geometries of the transition states, TS5A, TS5B, and TS5C, are shown in Figure 8. Again, the Gibbs free energy of activation for reaction 5A is higher than that for reaction 5B or 5C, depending on the pathway. We assumed that the Gibbs free energy of activation would also be higher in reaction 5A with R = $-C_6H_4-CH_3$ than in reaction 5B or 5C. The optimum structure of the transition state for reaction 5A with $Cp_2Ti(C_6H_4-CH_3)_2$ catalyst is shown in Figure 9. The activation parameters for reaction 5A are $\Delta H^‡ = 23.2$ kcal/mol and $T\Delta S^‡ = -8.8$ kcal/mol with R = $-C_6H_5$, and $\Delta H^‡ = 22.8$ kcal/mol and $T\Delta S^‡ = -9.8$ kcal/mol with R = $-C_6H_4-CH_3$ (see Table 7). These activation parameters are close to those for reaction 4A ($\Delta H^‡ = 22.5$ kcal/mol and $T\Delta S^‡ = -8.9$ kcal/mol). Therefore, the first activation Gibbs free energy ($\Delta G^‡$) by $Cp_2Ti(C_6H_4-CH_3)_2$ was 32.6 kcal/mol, which is very close to that (= 32.0 kcal/mol) by $Cp_2Ti(C_6H_5)_2$ or is slightly larger than that (= 31.5 kcal/mol) by $Cp_2Ti(CH_3)_2$. Therefore, ethene hydrogenation by $Cp_2Ti(C_6H_5)_2$ or $Cp_2Ti(C_6H_4CH_3)_2$ is expected to show reaction conditions similar to the σ bond metathesis mechanism by $Cp_2Ti(CH_3)_2$. From the above results, hydrogenation would proceed in the order

$$5A \rightarrow 5B \text{ (or } 5C \rightarrow 3A) \rightarrow 3D \ (\rightarrow 3A \rightarrow 3D)_n$$

or

$$5A \rightarrow 5B \text{ (or } 5C \rightarrow 3A) \rightarrow 3D \ (\rightarrow 3A \rightarrow 3B \rightarrow 3C)_n$$

Industrially, the hydrogenation reactions of unsaturated double bonds of the diene units on conjugated diene polymers and copolymers catalyzed by $Cp_2Ti(C_6H_5)_2$ and $Cp_2Ti(C_6H_4CH_3)_2$ are carried out in the range of 0 to 150 °C, or more preferably at 40 to 120 °C,[3b] which is in a larger temperature range than $Cp_2Ti(CH_3)_2$-catalyzed hydrogenation.

Conclusions

The mechanisms of ethene hydrogenation catalyzed by four different titanocene complexes were investigated by studying the kinetics and thermodynamics of possible reaction pathways. For the $Cp_2Ti(CO)_2$ catalyst, the hydrogenation reactions consist of first Ti−CO bond dissociation, second Ti−CO bond dissociation followed by the formation of Cp_2TiH_2, and then ethene hydrogenation by Cp_2TiH_2. The first three reactions are nonspontaneous (ΔG = 18.4, 12.8, and 7.4 kcal/mol). The Ti−CO bond dissociations of $Cp_2Ti(CO)_2$ have positive ΔSs, which means that the hydrogenation reactions take place at a higher temperature. Therefore, continuous heating of the system is necessary until the activation barrier of ethene hydrogenation by Cp_2TiH_2 is overcome. Experimentally, the $Cp_2Ti(CO)_2$-ctalyzed ethene hydrogenation takes place at 65 °C. Other hydrogenation reactions, Ti−CO bond dissociations of $Cp_2Ti(CO)_2$ (ΔG = 18.4 kcal/mol) and $Cp_2Ti(CO)(H_2)$ (ΔG = 18.8 kcal/mol), will take place much more slowly than the previous reaction pathways (first and second Ti−CO bond dissociations of $Cp_2Ti(CO)_2$ followed by the formation of Cp_2TiH_2).

For the $Cp_2Ti(CH_3)_2$ catalyst, the hydrogenation reactions consist of first σ bond metathesis ($\Delta G^‡ = 31.5$ kcal/mol) for the Ti−C(CH_3) bond and H−H bond, second σ bond metathesis ($\Delta G^‡ = 19.1$ kcal/mol), and then ethene hydrogenation by Cp_2TiH_2. Another hydrogenation begins with the first σ bond

Table 7. B3PW91-Computed Activation Parameters and Relative Thermodynamic Values (kcal/mol) in Reaction 5A ($Cp_2Ti(C_6H_4CH_3)_2$ Catalyst)

reaction 5A	$Cp_2Ti(C_6H_4CH_3)_2 + H_2$	$[Cp_2Ti(C_6H_4CH_3)_2(H_2)]^‡$	$Cp_2Ti(H)(C_6H_4CH_3) + C_6H_5CH_3$
ΔE	0	+21.4	−19.6
ΔE_0	0	+24.9	−15.7
ΔH	0	+22.8	−17.5
$T\Delta S$	0	−9.8	+4.6
ΔG	0	+32.6	−22.2

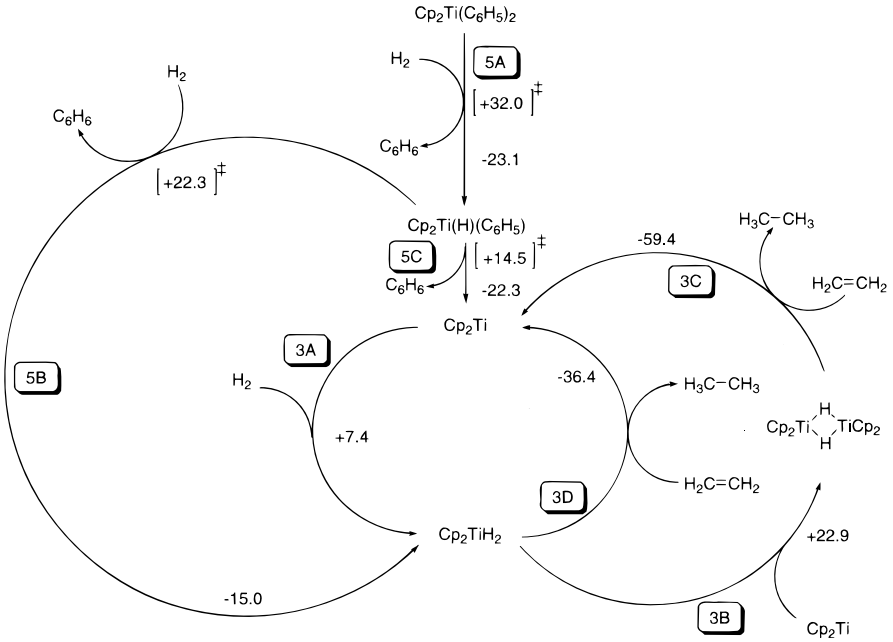

Figure 7. Gibbs free energy changes (kcal/mol) for reactions, 5A, 5B, 5C, 3A, 3B, 3C, and 3D computed by B3PW91. Values in [ ]‡ are Gibbs free energies of activation for corresponding reactions.

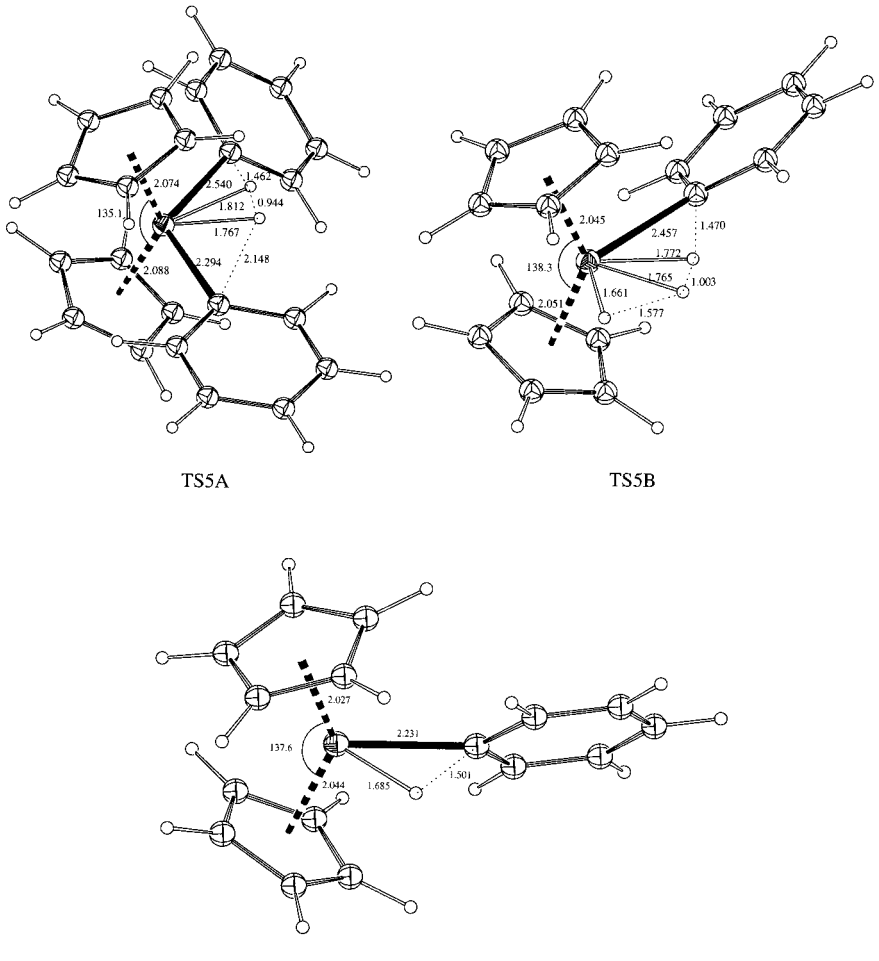

Figure 8. B3PW91-computed optimum geometries of transition states in reactions, 5A, 5B, and 5C ($Cp_2Ti(C_6H_5)_2$ catalyst).

metathesis ($\Delta G^{\ddagger} = 31.5$ kcal/mol), followed by the reductive elimination of methane to form Cp_2Ti ($\Delta G^{\ddagger} = 13.4$ kcal/mol), the formation of Cp_2TiH_2 ($\Delta G = 7.4$ kcal/mol), and then ethene hydrogenation by Cp_2TiH_2. Here, the first and second σ bond metathesis and the formation of Cp_2Ti proceed spontaneously ($\Delta G = -21.2$, -17.7, and -25.1 kcal/mol, respectively) and the ΔGs overcome the activation barriers of the subsequent reactions. Also, the ΔS for first σ bond metathesis is negative.

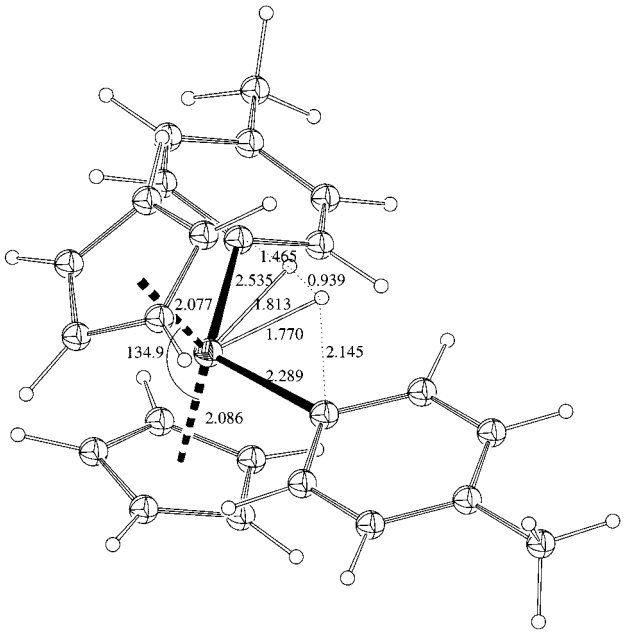

Figure 9. B3PW91-computed optimum geometries of a transition state in reaction 5A ($Cp_2Ti(C_6H_4CH_3)_2$ catalyst).

Therefore, the hydrogenation reactions by $Cp_2Ti(CH_3)_2$ take place below room temperature. Experimentally, the hydrogenation reaction takes place at 0 °C. Other pathways through α-H abstraction are also possible, but these pathways occur at a higher temperature.

For $Cp_2Ti(C_6H_5)_2$ or $Cp_2Ti(-C_6H_4CH_3)_2$, the hydrogenation consists of reactions similar to the σ bond metathesis for $Cp_2Ti(CH_3)_2$. The $\Delta G^{\ddagger}$s of first σ bond metathesis reactions for $Cp_2Ti(C_6H_5)_2$ and $Cp_2Ti(-C_6H_4CH_3)_2$ are, respectively, 32.0 and 32.6 kcal/mol, which are slightly larger than the $\Delta G^{\ddagger}$ value for $Cp_2Ti(CH_3)_2$. The σ bond metathesis reactions for $Cp_2Ti(C_6H_5)_2$ and $Cp_2Ti(-C_6H_4CH_3)_2$ are spontaneous. Their respective ΔGs of first σ bond metathesis reactions are −23.1 and −22.2 kcal/mol. This means that the activation barriers of the hydrogenation reactions, except for the first σ bond metathesis, can be overcome without heating. As with $Cp_2Ti(CH_3)_2$, the ΔSs for first σ bond metathesis reactions by $Cp_2Ti(C_6H_5)_2$ and $Cp_2Ti(-C_6H_4CH_3)_2$ are both negative. Therefore, hydrogenation reactions by $Cp_2Ti(C_6H_5)_2$ and $Cp_2Ti(-C_6H_4CH_3)_2$ take place at a lower temperature.

In the catalytic cycle, irrespective of the kind of catalyst, Cp_2TiH_2 or $(Cp_2TiH)_2$ hydrogenates ethene to form ethane and Cp_2Ti. The ethene hydrogenation by Cp_2TiH_2 occurs much faster than the formation of $(Cp_2TiH)_2$ from $(Cp_2TiH_2 + Cp_2Ti)$ followed by the ethene hydrogenation by $(Cp_2TiH)_2$. Since the ethene hydrogenation by Cp_2TiH_2 or $(Cp_2TiH)_2$ is spontaneous, the excess Gibbs free energy will increase the temperature of the system. As the catalytic cycle progresses, cooling the system will become necessary to avoid side reactions.

There are a few other reactions that were not investigated in this study, namely, possible transition states in the hydrogenation reactions of ethene by Cp_2TiH_2 in reaction 3D and $(Cp_2TiH)_2$ in reaction 3C. These reactions should be thoroughly reviewed. Solvent effects have also been ignored in this study. In addition to the mechanisms of simple bond dissociation, α-H abstraction, and σ bond metathesis described in this report, it is also possible for the hydrogenation catalysts to proceed by other mechanisms such as β-H elimination[33] or non-concerted reactions, which will be covered in future studies.

Acknowledgment. We would like to thank Professor John E. Bercaw at the California Institute of Technology for his useful discussion and references, Professor Pill-Soon Song at the University of Nebraska-Lincoln for proofreading the manuscript and helpful suggestions, and the Kumho Supercomputing Center staff for the use of computation time.

JA991799L

(33) (a) Togni, A.; Halterman, R. L., Eds.; *Metallocenes*; Wiley-VCH: Weinheim, 1998. (b) Sturia, S. J.; Kablaoui, N. M.; Buchwald, S. L. *J. Am. Chem. Soc.* **1999**, *121*, 1976 and references therein.